JOURNAL OF GEOPHYSICAL RESEARCH, VOL. 99, NO. D12, PAGES 25,857–25,868, DECEMBER 20, 1994

Radiation exchanges above West African moist savannas: Seasonal patterns and comparison with a GCM simulation

Xavier Le Roux,[1] Jan Polcher,[2] Gérard Dedieu,[3] Jean Claude Menaut,[1] and Bruno A. Monteny[4]

Abstract. During a field campaign of the Savannas on the Long Term (SALT) Global Change and Terrestrial Ecosystems/International Geosphere Biosphere Program dealing with the energy budget of a West African moist savanna, particular attention was paid to the radiation budget because it is the driving force for all other surface fluxes. All components of the radiation budget were measured on the ground during one and a half year on a test site in Ivory Coast. The seasonal variations of the observed radiation at the surface and satellite data were compared to the values simulated for the 1978-1988 period by a general circulation model coupled to a land surface parameterization scheme, both developed by the Laboratoire de Météorologie Dynamique (LMD). Problems which appear when point observations of surface fluxes are compared with results from general circulation model simulations are addressed. Seasonal variations of the prescribed savanna albedo in the model differed significantly from the observed variations due to bush fire influence. However, the major discrepancy between model simulations and surface observations resulted from the overestimation of the incoming shortwave radiation at the surface. The major sources of discrepancy were found to be the simulated clear-sky atmospheric absorption and/or scattering of the shortwave radiation and the simulation of cloud and/or cloud-radiation interactions which lead to an overestimation of the absorbed energy at the surface by the model. It is concluded that improvement of the simulated energy budget in the humid tropics depends critically on a good simulation of the incoming shortwave radiation at the surface.

1. Introduction

Both local climate and ecosystem functioning are primarily driven by the energy absorption and partitioning at the surface and thus by surface radiative and hydrological properties. Over the past decade, there has been an increasing awareness that interactions between land surfaces and the atmosphere may also influence the global climate system. This has prompted research to improve land surface characterization and modeling in order to assess realistic momentum, mass, and energy exchanges between the surface and the atmosphere as boundary conditions for general circulation models (GCMs) [e.g., *Dickinson et al.*, 1986, *Sellers et al.*, 1986, *Ducoudré et al.*, 1993]. Several global data bases have been proposed to improve the specification of surface albedo or other surface parameters in GCMs. Numerical experiments with these models have demonstrated the sensitivity of atmospheric circulation and rainfall patterns to the representation of land surface processes (e.g., as reviewed by *Mintz*, [1984]). Albedo, roughness, and biophysical control of evapotranspiration have been identified as key surface parameters. Furthermore, changes in the surface radiation budget and particularly in the surface albedo caused by anthropogenic activities (see *Gornitz and NASA*, [1985] for West Africa) have been proposed as a potential cause of climatic variation [e.g., *Charney et al.*, 1977]. Therefore an adequate characterization of the surface radiation budget is the prerequisite of a realistic and accurate representation of the energy exchanges between the continental biomes and the atmosphere. Tropical areas are especially important in this context, as the energy absorbed at the surface and its restitution to the atmosphere is a major driving force for the general circulation. Comprehensive information on the radiative and energetic exchanges between the tropical biomes and the atmosphere is needed. But such published data are scarce and only tropical moist forests

[1] Ecole Normale Supérieure (ENS) Laboratoire d'Ecologie, CNRS, Paris.
[2] ENS, Laboratoire de Météorologie Dynamique du CNRS, Paris.
[3] LERTS, Unité mixte CNES-CNRS, Toulouse, France.
[4] Laboratoire de Bioclimatologie, ORSTOM, Montpellier, France.

Paper number 94JD01526.
0148-0227/94/94JD-01526$05.00

[*Pinker et al.*, 1980, *Shuttleworth et al.*, 1984, *De Abreu et al.*, 1988, *Shuttleworth*, 1988, *Monteny and Casenave*, 1989] and steppe like savannas of African semi arid regions [*Van de Griend et al.*, 1989, *Gash et al.*, 1991] have been studied. The radiative and energetic exchanges above most of the savanna biome remain unknown. The only data reported for mesic and moist savannas are limited to Oguntoyinbo's work [*Oguntoyinbo*, 1970] which presents albedo values for different types of vegetation in Nigeria (West Africa) with crude temporal variations of this parameter. According to *Andreae* [1991], savannas cover at least 15×10^6 km^2, an area of the same order as the area covered by tropical forests (14×10^6 km^2). Undoubtedly, exchanges between savannas and the atmosphere influence significantly the regional and global climate. This is particularly true for West African savannas which cover about 3×10^6 km^2, all in one block [*Menaut et al.*, 1991].

A major recommendation for GCMs improvement is to study the simulation of the surface energy balance in a range of models for different land surfaces, with detailed comparisons with suitable observations [*Garratt*, 1993, *Garratt et al.*, 1993]. Two types of observations are available in this context: remote sensing data and in situ measurements. Each one has its specific advantages when used to test the outputs of a GCM. Satellite measurements cover surfaces commensurate with the area of a GCM grid box. The main drawback is that not all surface fluxes are accessible and that accuracy is low. On the contrary, point observations allow a comprehensive and accurate description of the components of the surface energy budget. However, the significance of point measurements for the area of a GCM grid box remains to be determined. The objective of this paper is to compare original local measurements of the seasonal variations of the radiation exchanges above a moist savanna to values simulated by a GCM. Data were collected in Ivory Coast (West Africa) between January 1991 and May 1992 and consist of radiation measurements during 258 complete daily cycles. Routine observations of incoming solar radiation and precipitation during an 11-year period at the test site, and satellite data were also used. All these data were compared to values simulated by the general circulation model developed by the Laboratoire de Météorologie Dynamique (LMD-GCM) [*Sadourny and Laval*, 1984] coupled with the SECHIBA surface biome scheme [*Ducoudré et al.*, 1993]. Firstly, the discrepancies in the downward radiation and their sources are analyzed. Secondly, the difference in absorbed energy at the ground is discussed by taking into account the sub grid variabilities of surface properties.

2. Field Measurements

2.1. Test Site

West African vegetation is roughly organized in stripes corresponding to a positive gradient of humidity from the Sahara to the Gulf of Guinea [*White*, 1986]. The savanna biome encompasses the Sahel zone, or arid savannas, the Sudan zone which includes dry forests and wooded savannas, and the Guinea zone with a transitional forest-savanna mosaic. The Guinea savanna zone can be defined as a zone of dense and high-grass layer dominated by scattered trees where the mean annual precipitation exceeds 1000 mm and where the dry season lasts less than two months [*Menaut*, 1983]. In central West Africa, Guinea savannas extend north of the tropical forest area to 9°N and cover roughly 0.5×10^6 km^2 [*White*, 1986].

This study was conducted at the Lamto Scientific Station (6°13′ N, 5°02′ W), in a typical Guinea savanna of Ivory Coast. The test site is a shrubby savanna with a lower vegetation layer consisting mainly of grass species dominated by *Andropogon* sp. and *Hyparrhenia* sp. and of low shrubs (height < 2 m) and an upper layer ($2 <$ height < 6 m) consisting of shrubs dominated by *Cussonia barteri*, *Crossopteryx febrifuga*, and *Bridelia ferruginea* (14.7% cover when fully developed). Detailed ecological site description may be found in the work of *Menaut and César* [1979].

The climate is sub equatorial with two contrasted seasons. Temperatures are quite constant all year long (monthly means range from 25.4° to 31.2° C). Annual precipitations average 1210 mm and range from 800 to 1690 mm for the 1962-1990 period. Well-defined precipitation periods occur: a long dry season in December and January, and a long rainy season from February to November, usually interrupted by a short dry period in August. Savanna fires occur each year during the dry season, generally in January, and consume much of the grass layer. Figure 1 presents the monthly precipitations during the study period (from January 1991 to May 1992). A marked dry season occurred from December 1991 to February 1992. Annual precipitation was 1180 mm in 1991 and only 990 mm in 1992. Figure

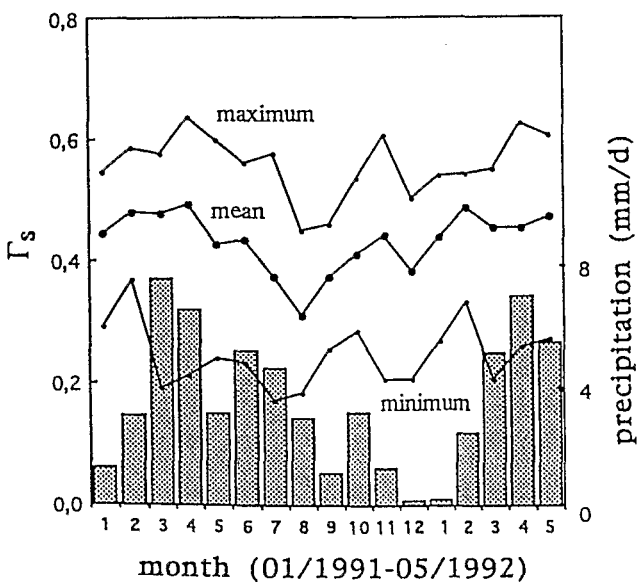

Figure 1. Seasonal variations of the monthly precipitation (right scale) and of the maximum, minimum, and mean of the daily ratio (Γ_s) between shortwave radiation at the surface and at the top of the atmosphere (left scale) observed in Lamto.

1 also presents monthly mean, maximum and minimum of the fraction (Γ_s=$R_{s\downarrow}/R_o$) of extraterrestrial incoming shortwave radiation (R_o) that reaches the ground ($R_{s\downarrow}$) and can be used for land surface processes. Γ_s ranged from 0.2 during very cloudy periods to 0.65 during clear periods. The monthly mean Γ_s was maximum from February to April and minimum from July to September due to the stratiform clouds which occur when the intertropical convergence has moved far north in West Africa. It was relatively low in December 1991 because of high atmospheric aerosol loading associated with northern winds.

When presented for a specific year, the monthly mean values are averages of the daily values, else averages of monthly means from the available years are used.

2.2. Radiation Measurements

Routine meteorological and radiative measurements were provided by an automatic station controlled by a data logger (Campbell CR10). The radiation budget is given by

$$R_n = (1-a)R_{s\downarrow} + R_{l\downarrow} - R_{l\uparrow} \qquad (1)$$

where R_n is the net radiation (Wm^{-2}), $R_{s\downarrow}$ is the downward shortwave radiation (Wm^{-2}), a is the surface albedo, $R_{l\downarrow}$ is the downward longwave radiation (Wm^{-2}), and $R_{l\uparrow}$ is the upward longwave radiation (Wm^{-2}) which takes into account the emitted radiation and the reflected $R_{l\downarrow}$. Sample measurements at 30-s intervals were used to provide 20-mn average values of downward shortwave radiation (Skye Instruments pyranometer at a height of 2 m in an open area), upward shortwave radiation (downward facing Skye Instruments pyranometer mounted at a height of 8.5 m), upward longwave radiation (downward-facing Everest Interscience, chopped infrared thermoradiometer mounted at a height of 10 m), and net all-wave radiation (two Campbell Q6 net radiometers mounted at a height of 3 and 8.5 m). The downward longwave radiation was not measured directly at the site but was obtained as the residual term of equation (1). Another thermoradiometer was used as a reference. The instruments were mounted on a mast accurately leveled at the end of 2-m booms orientated in a way to minimize any interference by the mast shade. Screen air temperature (copper/constantan thermocouple) and water vapor pressure (Kroneis dew point sensor) were also measured routinely. The station was run continuously from January 1991 to June 1991 and from October 1991 to May 1992. No data were collected during the summer months.

Before the study, infrared thermoradiometers were calibrated in France above a cropped surface. After the study the calibration was checked against a hemispheric blackbody. The measurements produced by the two pyranometers, the two net radiometers, and the two infrared thermoradiometers agreed within systematic errors of 1.5, 1, and 4%, respectively. During the study the measurements produced by the pyranometers and a Kipp and Zonen reference pyranometer agreed within errors of 1%. Skye Instruments pyranometers feature a silicon photovoltaic sensor. They are calibrated for downward shortwave radiation and should not be used a priori for reflected shortwave radiation measurements. We verified, however, that the albedo measured with Skye Instruments and Kipp and Zonen pyranometers agreed within systematic errors less than 4%. The measurements produced by the net radiometers mounted at a height of 8.5 and 3 m, respectively, agreed within systematic errors of 3% during the study period. As the net radiometer mounted at 8.5 m high was connected to a data logger providing only diurnal measurements of energy partitioning, only the net radiation measured by the other net radiometer was used for this study.

The radiation budget was established in an open area, above a soil-grass-low-shrub system, away from high shrubs. However, albedos of shrubby (with high and low shrubs) and open (with only low shrubs) areas were found to be similar (H. Gauthier and X. Le Roux, unpublished data 1994); thus the observed albedo can be assumed to be representative of the test site. We assume also that the high shrubs do not drastically influence the upward longwave radiation at the test site scale because their fractional cover is low enough and because the phenology of the shrub species follows roughly that of the grass species in Guinea savannas (same defoliation and growing periods). This assumption can be questionable in drier savannas [e.g,. *Van de Griend et al.*, 1991] where $R_{l\uparrow}$ can be very different for a nearly bare soil or fully developed shrubs.

2.3. Verification of the Radiation Balance Closure

To verify the closure of the radiation balance, the downward longwave radiation was independently estimated with the empirical expression proposed by *Brunt* [1932]:

$$R_{l\downarrow}^{cal} = (\alpha + \beta e^{0.5})\sigma T^4 \qquad (2)$$

where $R_{l\downarrow}^{cal}$ is the calculated downward longwave radiation (Wm^{-2}), T is the air temperature at screen level (K), e is the water vapor pressure at screen level (mbar), σ is the Stefan-Boltzmann constant (5.67×10^{-8} $Wm^{-2}K^{-4}$), and α and β are empirical constants equal to 0.605 and 0.048 in the modified expression proposed by *Sellers* [1965].

Figure 2 compares the measured net radiation R_n^{mes} and the calculated net radiation R_n^{cal}, sum of the measured downward and upward shortwave radiation, the measured upward longwave radiation, and the downward longwave radiation calculated by the Brunt formula (2) with empirical parameters proposed by *Sellers* [1965]. The simple specification of the downward longwave radiation provided a very good calculation of the net radiation. It is illustrated here with two diurnal periods, one representative of oceanic air mass condi-

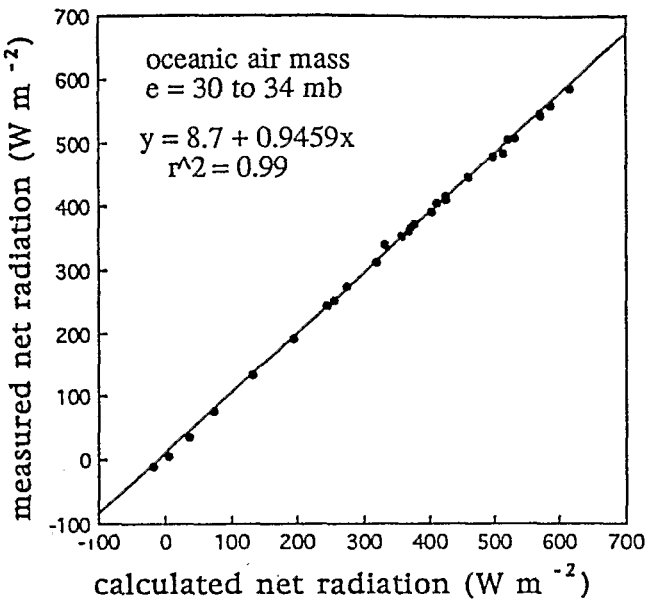

Figure 2. Comparison of the measured and calculated net radiation for a diurnal period representative of oceanic air mass conditions (water vapor pressure e ranging from 30 to 34 mbar).

tions (Figure 2) and another of continental air masses (Figure not shown).
Oceanic air mass conditions ($30 < e < 34$ mbar):

$$R_n^{mes} = 0.946 R_n^{cal} + 8.7 \quad r^2 = 0.99 \qquad (3)$$

Continental air mass conditions ($16 < e < 22$ mbar):

$$R_n^{mes} = 1.003 R_n^{cal} + 3.4 \quad r^2 = 0.99 \qquad (4)$$

This shows that both methods are consistent and that $R_{l\downarrow}$ estimated as the residual in equation (1) provides a reliable estimation of the atmospheric longwave radiation.

3. Laboratoire de Météorologie Dynamique (LMD) General Circulation Model: Description and Outputs

The simulation used here was conducted with the LMD atmospheric GCM described by *Sadourny and Laval* [1984] and *Laval and Picon* [1986], coupled to the surface processes model SECHIBA [*Ducoudré et al.*, 1993]. The model used for this study is a version of cycle 5 [*Polcher et al.*, 1991] which includes the diurnal cycle [*Polcher and Laval*, 1994]. The LMD-GCM is a grid point model discretized regularly in longitude (64 points) and in sine of the latitude (50 points) and irregularly along the vertical axis (11 sigma levels). Near the equator, each point represents roughly a 2° by 6° box. The shortwave radiation scheme used in the model [*Fouquart and Bonnel*, 1980] takes into account absorption and scattering by water vapor, carbon dioxide, and ozone as well as by cloud droplets. The longwave radiation was computed by the scheme proposed by *Morcrette et al.* [1986]. Radiation interacted with the clouds computed by the prognostic scheme implemented by *Le Treut and Li* [1991]. The cloud scheme was called every 30 min and the radiation code was applied every 2 hours. For each grid box of the model, eight land surface types were defined (bare soil plus seven vegetation classes), each of them covering a fractional area of the grid box, as determined from the atlas of *Matthews* [1984] [see *Ducoudré et al.*, 1993]. The latent heat flux was computed independently for each of these covers and then averaged over the grid box. The surface energy budget was computed for the entire grid box because albedo and roughness length were averaged over it. These values were prescribed each month from the climatology proposed by *Dorman and Sellers* [1989] and interpolated to the GCM grid boxes.

The GCM results for the 11-year period (1978-1988) were taken from the control case of a deforestation experiment [*Polcher and Laval*, 1994]. To have a realistic interannual variability, the model was forced with the observed sea surface temperatures. Lamto is located at the boundary of two grid boxes of the GCM. The upper one (6°30′ – 9°10′N, 0° – 6°W) was chosen because its dominant vegetation type is moist savannas and the simulated precipitation pattern corresponds to a sub equatorial climate. The vegetation prescribed in this box consists of 52% of savannas, 26% of tropical rain forests, 19% of steppe like vegetations, 2% of evergreen forests, and 1% of bare soil. The annual mean precipitation simulated by the GCM for the 1978-1988 period was not significantly different from that in Lamto (1162±145 and 1228±142 mm, respectively; p =0.5%). As observed in Lamto (Figure 3), the model simulates

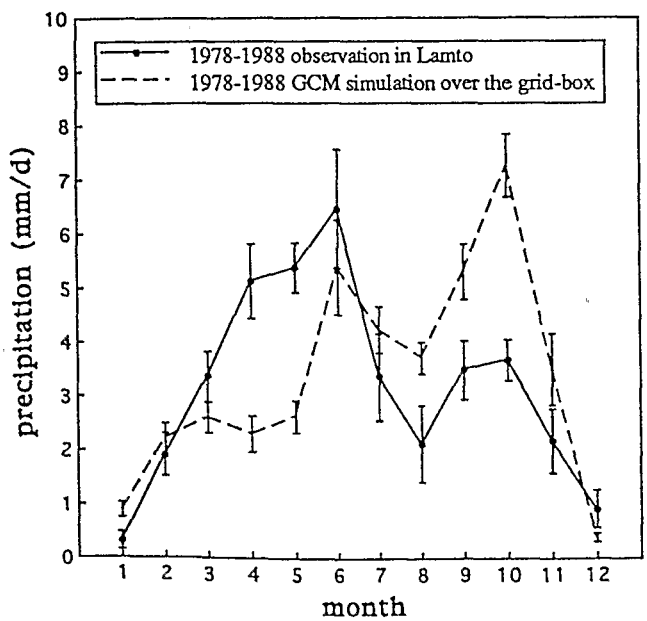

Figure 3. Comparison between the annual variations of the monthly precipitation observed in Lamto and the values simulated by the general circulation model of the Laboratoire de Météorologie Dynamique, both for the 1978-1988 period. Bars are standard errors.

a marked dry season in December and January, and a rainy season with maxima in June and October, interrupted by a relative dry period in August. However, discrepancies can be noted on the intensity of the rainy periods: the first one is underestimated and the second one overestimated. The largest discrepancy occurred in October.

4. Other Data Sets

Daily solar radiation and daily precipitation data obtained at the Lamto Geophysical Station were used for the present study. Since 1977, daily solar radiation was routinely measured with a Gun Bellani pyranometer. It was verified that the daily solar radiation measured by this pyranometer compared well with our daily integrated solar radiation values measured from January 1991 to May 1992, and the following calibration was applied to the Lamto Station solar radiation data:

$$R_{s\downarrow} = 0.952 R_{s\downarrow}^{Gun} + 7.87 \qquad r^2 = 0.95 \qquad (5)$$

where $R_{s\downarrow}$ is the daily downward shortwave radiation (Wm^{-2}) and $R_{s\downarrow}^{Gun}$ is the daily downward shortwave radiation measured by the Gun Bellani pyranometer (Wm^{-2}). Precipitation has been routinely measured at the Lamto Station since 1962.

Radiation data obtained for the year 1988 by the Earth Radiation Budget Experiment (ERBE) [*Barkstrom and Smith*, 1984] were used, averaged over the GCM grid box. Special attention was paid to the radiative impact of clouds on the shortwave radiation budget of the Earth-atmosphere system, namely the shortwave cloud radiative forcing CRF_{sw}, which is defined as

$$CRF_{sw} = R_o(a_c - a) \qquad (6)$$

where R_o is the incoming shortwave radiation at the top of the atmosphere and a_c and a are the planetary albedo for clear-sky conditions and all conditions, respectively. Clear-sky radiation was calculated by the GCM regardless of whether clouds were actually simulated, by not taking into account cloud effect. The CRF_{sw} is negative and represents a cooling effect of clouds on the Earth-atmosphere system. This variable is directly measurable from space and constitutes a useful tool to analyze cloud representation in the GCM.

Two albedo data sets [*Matthews*, 1984;*Dorman and Sellers*, 1989] widely used for global climate modeling and available on $1° \times 1°$ global grids were used in this study. From these climatologies the two boxes located between $7° - 8°$N and $4° - 6°$W were used. They correspond to the "grassland with shrub cover" vegetation in the atlas of *Matthews* [1984] and to "broadleaf trees with ground cover (savanna)" vegetation for *Dorman and Sellers* [1989].

Surface bidirectional reflectances over the grid box considered here were obtained from Meteosat data for the years 1984 and 1985. The method used to derive them has been described in detail by *Dedieu et al.* [1987] and its accuracy discussed by *Arino et al.* [1991]. The method involves the following steps: (1) cloud screening using a minimum shortwave reflectance ($0.35 - 1.1\,\mu$m) compositing technique [*Arino et al.*, 1991]; (2) calibration of raw digital counts, giving top of the atmosphere (TOA) radiances; (3) normalization of radiances by solar irradiance to compute TOA reflectance; (4) correction of atmospheric effects based on climatologies, to obtain surface bidirectional reflectances [*Rahman and Dedieu*, 1994]. A sampling process which selects one 6×6 km^2 pixel from each 30×30 km^2 area (Meteosat International Satellite Cloud Climatology Project B2 product supplied by ESA/ESOC) has been applied. Monthly composites are derived from images acquired during one month at 1130 UTC. This procedure eliminates most of cloud contamination, except during summer months in the humid savanna zone where nearly permanent cloud cover occurs.

5. Comparison of GCM Outputs With in Situ and Satellite Measurements

5.1. Downward radiation

Observed incoming radiation integrates the signal from a large part of the hemisphere above the surface. Such observations are representative of an area much larger than the test site. Averaging downward radiation over a month ensures that the result is independent of small-scale meteorological phenomena and is compatible with values computed in a GCM for a relatively large grid box. Thus it is legitimate to compare monthly mean observations of incoming radiation with output from a climate model.

Downward shortwave radiation. Figure 4 presents the average seasonal variations over the 1978-1988

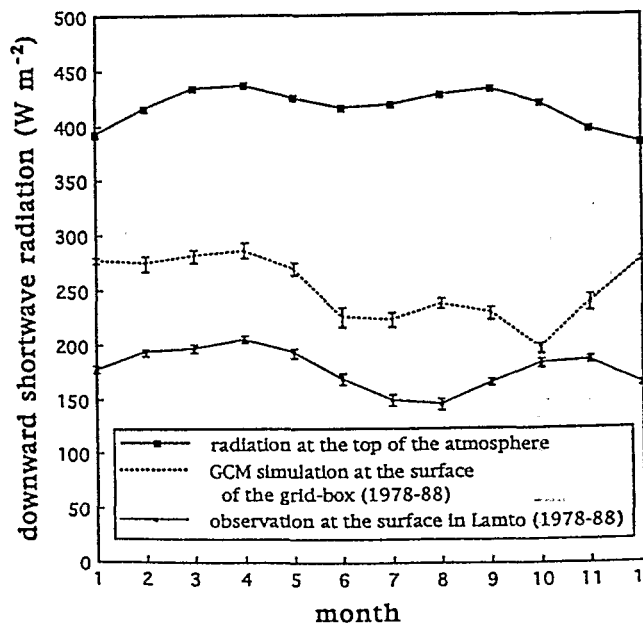

Figure 4. Average annual variations in the monthly downward shortwave radiation observed in Lamto and simulated, both for the 1978-1988 period. Bars are standard errors.

period of the downward shortwave radiation: at the top of the atmosphere, observed at the surface in Lamto and simulated at the surface by the LMD-GCM over the grid box. The observed monthly mean fraction of extraterrestrial shortwave radiation which reaches the ground (Γ_s) ranged from 0.45 to 0.48, except in the middle of the rainy season, particularly in August when the mean Γ_s decreased to 0.33, and except in December and January when it was below 0.45. The corresponding monthly mean downward shortwave radiation ranged from 205 Wm^{-2} in April to 145 Wm^{-2} in August. Low Γ_s during the short dry season (August) are linked to the movement of the intertropical convergence zone far north of our study site. During this season, insolation is very low due to a more or less continuous cover of stratiform clouds. The December-January minimum occurs when the intertropical convergence zone lies 5°N. During these almost cloudless months the dust mass in the atmosphere becomes important and increases the attenuation of the direct solar beam even in southern Ivory Coast as shown by *Monteny and Gosse* [1978].

Figure 4 shows that the incoming shortwave radiation at the surface is largely overestimated by the LMD-GCM. The annual fraction of extraterrestrial incoming shortwave radiation reaching the ground Γ_s measured in Lamto and simulated by the GCM in the Guinea zone was 0.42 and 0.61, respectively. Table 1 shows that the observed value is similar to those measured in five other locations in southern Côte d'Ivoire [*Monteny*, 1987] and close to the ones measured in other sub equatorial regions. Such low values are explained by the important cloud cover in equatorial and sub equatorial regions. The value simulated by the model (0.61) is close to Γ_s measured in the West African Sudan zone or Sahelian-Sudan zone where the winter months are nearly cloudless. The high Γ_s simulated by the model lead to an overestimation of the annual incoming solar energy at the surface by 43% (252 Wm^{-2} against 176 Wm^{-2} observed per year for the 1978-1988 period). Is this discrepancy the result of a poor simulation in the model of cloud cover or albedo and of clear-sky radiation, or of the lack of aerosol effects?

Figure 5 shows that the shortwave cloud radiative forcing simulated by the LMD-GCM generally agreed well with the cloud forcing observed at the top of the atmosphere. In August the simulated cloud forcing was too low (in absolute values) which is consistent with the relatively high Γ_s simulated at this time compared to observations (Figure 4). In October the simulated cloud forcing was higher (in absolute values) than the observed forcing. During this month the model produced too much convection (Figure 3) and an ensuing low Γ_s (Figure 4). Nevertheless, the shortwave cloud radiative forcing was correctly simulated during all the remaining months. Thus errors in the reflection of the shortwave radiation by clouds cannot account for the high incoming shortwave radiation simulated at the surface by the LMD-GCM. Note that the excess of incoming shortwave radiation at the surface in the simulation did not induce an excess of upward shortwave radiation detected at the top of the atmosphere (Figure 5). This is explained by the fact that for an excess of shortwave radiation reaching the surface of the order of 70 Wm^{-2}, the expected excess of upward shortwave radiation at the top of the atmosphere is only of the order of 9 Wm^{-2} after reflection by the surface and transmission in the atmosphere.

Figure 6 compares the clear-sky downward shortwave radiation at the surface simulated by the model and the observed clear-sky radiation. Ground-based values of clear-sky radiation were obtained by selecting the absolute maximum value of daily surface radiation for each month over the 1978-1988 period. It was assumed that this value could represent roughly the clear-sky radiation for the month, except from July to September when fully cloudless days never occurred, which explains the relatively low maximum values. On the other hand, the GCM clear-sky radiation was a monthly mean calculated in the model by disregarding clouds in the radiation code. The effect of higher atmospheric water vapor content associated with cloud occurrence is not removed by this method. Avoiding this bias would only increase the clear-sky downward shortwave radiation. Furthermore, this effect did not exist in December and January when the model simulated almost no clouds (Figure 5). Figure 6 reveals that the absorption and scattering of shortwave radiation by the clear-sky atmosphere was underestimated by the model, which lead to an overestimation of the downward shortwave radiation of the order of 20 to 25%. This is a major reason explaining the discrepancy between all-sky conditions observed and simulated incoming shortwave radiation.

Table 1. Published Values of the Ratio Between Incoming Shortwave Radiation at the Surface and the Top of the Atmosphere for Different Tropical Locations and the Ratio Simulated by the General Circulation Model of the Laboratoire de Météorologie Dynamique (LMD-GCM)

Zone	Γ_s	Location	Authors
Equatorial forest	0.48	Kinshasa-Congo	*Monteith* [1972]
	0.40	Manaus-Amazonia	*Shuttleworth et al.* [1988]
	0.40-0.45	southern Ivory Coast	*Monteny*, [1987]
Guinea zone	0.42	Lamto-Côte d'Ivoire	this study
Sudan zone	0.58	Samaru-Nigeria	*Monteith* [1972]
Sahel	0.62	Banizoumbou-Niger	*Monteny* [1992]
Simulation for the Guinea zone	0.61	grid box in Guinea zone	LMD-GCM, this study

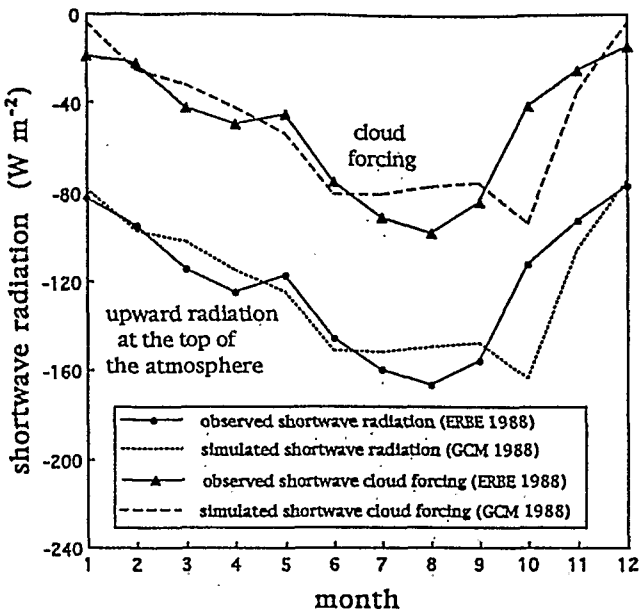

Figure 5. Annual variations of the upward shortwave radiation and of the shortwave cloud radiative forcing observed during the Earth Radiation Budget Experiment (ERBE) and simulated by the LMD-GCM, both in 1988 over the GCM grid box.

This discrepancy has two major sources: (1) The absorption and/or scattering of shortwave radiation by water vapor and ozone in clear-sky conditions (Figure 6) depends on the shortwave radiation parameterization used in the model, and on the simulated profiles of the absorbers in the atmosphere. The latter is probably the major factor since the shortwave radiation codes have been accurately validated. *Bony* [1993], for example, has shown for several GCMs that the integrated atmospheric water content is strongly underestimated in the tropics. (2) The absorption and scattering of aerosols was not taken into account. The former could reinforce the discrepancy between the observed and the simulated values particularly in December and January (Figure 4), since during these two generally cloudless months, the atmospheric aerosols loading is often high.

The discrepancy may also be attributed to errors in the transmissivity of the cloudy systems which is a function of the simulated liquid water content, the prescribed droplet size, and the type of clouds simulated. A correct albedo for the simulated cloudy systems does not imply a realistic transmissivity.

Downward longwave radiation. Figure 7 compares the seasonal variations in the monthly mean downward longwave radiation calculated with the observations available from January 1991 to May 1992 and simulated by the GCM for the 1978-1988 period. The observed monthly radiation ranged from 410 to 435 Wm^{-2}, with minima observed in December and January and maxima during the rainy season. The lower values are probably explained by lower water vapor content of the continental air masses and higher values by the importance of the cloud cover. The observed values were close to the downward longwave radiation reported by *Shuttleworth et al.* [1984] above the Amazonian forest in September (412 Wm^{-2}). Figure 7 shows that the downward longwave radiation at the surface simulated by the LMD-GCM was lower than the observed radiation, but that the simulated seasonal variation of this radiation was close to the observed one. Both observed and simulated seasonal patterns exhibited minima during the dry season in December and January, corresponding to continental air mass conditions. The low values simulated by the model were consistent with the high Γ_s because a low atmospheric shortwave radiation absorption would lead to a cooler atmosphere and thus to a lower longwave radiation emission.

5.2. Absorbed Radiation at the Surface

Theoretical considerations. Comparing point observations of variables linked to land surface processes to outputs of a general circulation model is an exceedingly important but difficult endeavor. Measurements are representative of a plot of approximately a few hectares or less, but the land surface scheme of a climate model is designed to take into account an ensemble of landscapes. However, in situ observations are still the most obtainable and reliable source of measurements of land surface parameters and fluxes and hence it is necessary to derive a method to use these data for the validation of general circulation model outputs.

If we wish to compare statistically a variable computed by the GCM with a set of observations, we need to take into account their statistical distribution over time and space to determine the probability of a mismatch. Land surfaces of the size of a GCM grid box may encompass a great variety of biomes and soil prop-

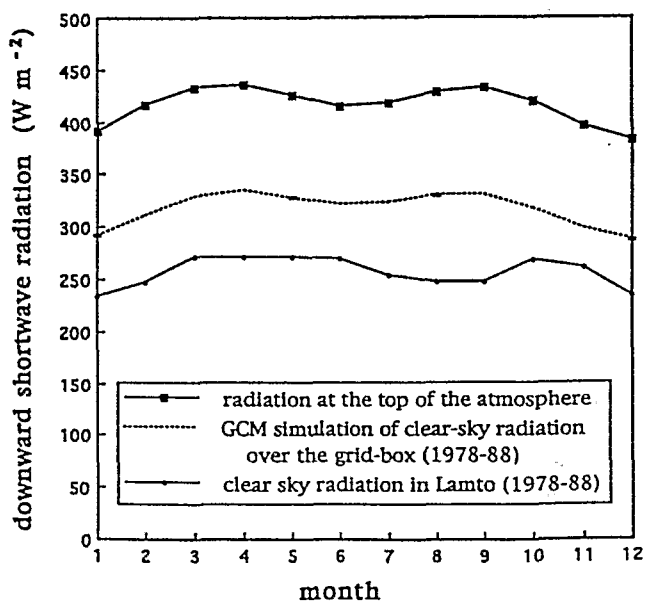

Figure 6. Average annual variation of the downward shortwave radiation (1) at the top of the atmosphere, (2) simulated at the surface in clear-sky conditions by the LMD-GCM, and (3) observed in Lamto in clear-sky conditions, all for the 1978-1988 period.

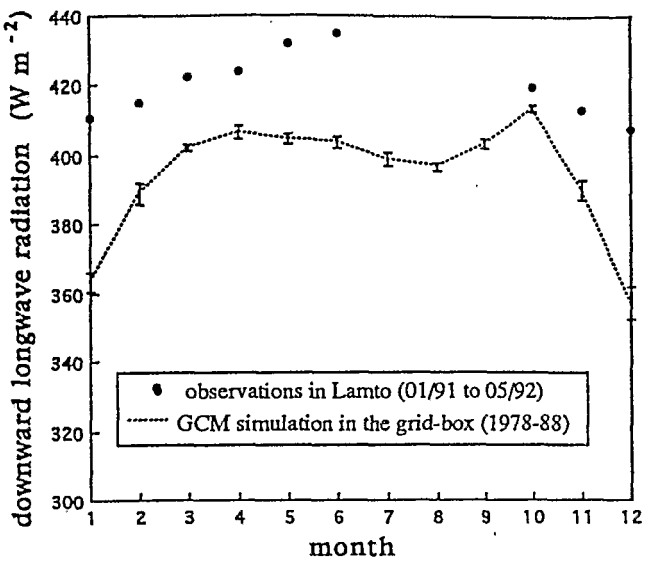

Figure 7. Annual variations of the downward longwave radiation observed from January 1991 to May 1992 and simulated by the LMD-GCM for the 1978-88 period. Bars are standard errors.

erties. This leads to a high variability of surface parameters and fluxes. Point measurements will follow, for the area considered, a complex distribution. It will be multimodal and probably not symmetric and may lead to failure of most statistical tests (for instance, the t-test or Wilcoxon test). This means that even with a very complete data set over the GCM grid box a comparison is difficult.

A potential solution to this problem is to divide this area into typical biomes and soil types. This will lead to simple distributions of the surface parameters and fluxes around the mean values. Surface fluxes computed with mean parameters for the grid box have to be replaced by an average of the fluxes determined for each biome. It can be achieved with an algorithm which calculates an energy balance for each surface type. The model will then yield fluxes representative of a biome for which we have observations with a known variability. A sound statistical comparison can then be done.

We are not yet able to proceed this way for all surface fluxes because the GCM does not yet contain the sub grid scale variability of fluxes, but we can use the method in the relatively simple case of absorbed radiation at the surface. As in this case, the relation between the surface property (albedo) and absorbed energy is linear and the albedo known for each biome, we can deduce the values the model would compute over savannas, if we assume that the measurements done in Lamto are representative of West African moist savannas.

Surface albedo. Figure 8 compares the observed seasonal trend of the savanna surface albedo in Lamto to the seasonal patterns prescribed in the GCM over the grid box and given for Guinea savannas by two albedo data sets widely used for global climate modeling [*Matthews*, 1984, *Dorman and Sellers*, 1989]. The observed monthly surface albedo increased from low values (0.075 and 0.11 in January 1991 and 1992 respectively) strongly influenced by the low albedo of the bare black soil after the fire occurrence to 0.23 when the canopy was fully developed. At the end of the annual vegetation cycle, albedo was approximatively 0.19 and no clear influence of senescence was observed. The seasonal trend of the albedo prescribed over the GCM grid box cannot be easily compared to that observed in Lamto because of the sub grid scale variability. This can be taken care of by comparing the grid box albedo with the original value for savannas computed by *Dorman and Sellers* [1989].

The seasonal trend of the surface albedo proposed by *Dorman and Sellers* [1989] for Guinea savannas was weak and opposite to the observed one in Lamto at the beginning of the year and remains nearly constant all year long. Nevertheless, the prescribed annual albedo was close to the observed one: 0.187 and 0.194, respectively. The climatology proposed by *Matthews* [1984] reproduced a seasonal trend that is in better agreement with observations. In fact, the annual cycle of albedo exhibited by Guinea savannas in the climatology of *Dorman and Sellers* [1989] was not appropriate because a major perturbation occurring each year in the African savannas was not taken into account, namely, savanna fires. Savanna fires, almost all resulting from human activities, result in a strong seasonal trend of albedo (Figure 8) related to the darkening of the surface after fire and to the marked seasonal variation of the vegetation fractional cover. Such an important phenological trend has not been integrated in the climatology. It may be asked if using the climatology of *Dorman and Sellers* [1989] in a GCM will induce an error of the grid box albedo, considering the diversity of biomes at this scale. The question can be answered with remote sensing data.

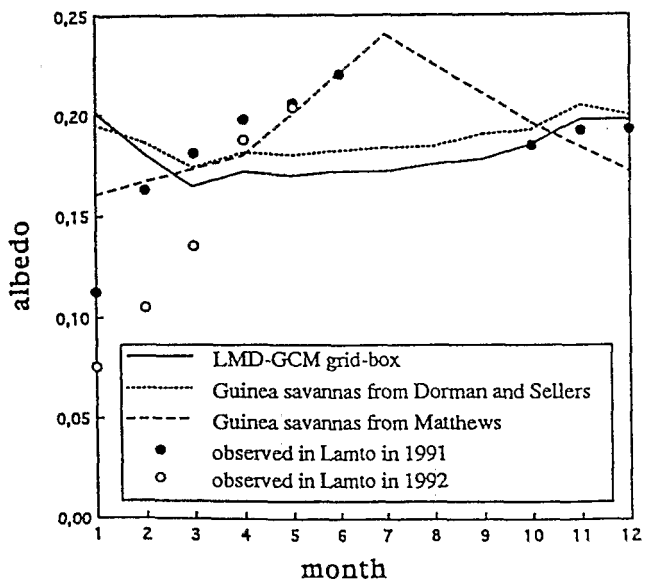

Figure 8. Comparison between the annual variations of surface albedo: (1) observed in Lamto from January 1991 to May 1992, (2) prescribed in the LMD-GCM over the grid box, (3) given for savannas by *Dorman and Sellers* [1989], and (4) by *Matthews* [1984].

Meteosat bidirectional reflectance (Figure 9) over the GCM grid box exhibits a large seasonal trend which agrees with the one observed for albedo in Lamto. This seasonal cycle can hardly be explained either by remaining cloud cover which essentially affects summer months values, as indicated by the standard error induced by the spatial variance during this period, or by surface directional effects. The low values obtained during the dry season can be explained by the occurrence of savanna fires. We conclude that this annual perturbation does strongly influence the seasonal pattern of albedo on an area commensurate with a GCM grid box in the humid savanna zone.

The monthly mean values presented in Figure 9 result from complex distributions, as can be seen for the month of January in Figure 10. Even at a 6 × 6 km resolution, the probability density of bidirectional reflectance is multimodal, which illustrates the heterogeneity of land surface types and burning within the grid box. The probability density shows that a mean value of surface reflectance at the grid-scale has no clear meaning. The statistical significance of an albedo over the grid box cannot be determined, but it must be considered in relation to the different modes of the distribution and, in fact, to the surface types. The mean values observed in January for 1984 and 1985 are associated to different distributions of the bidirectional reflectance caused by a varying impact of savanna fires. The peak centered around 0.09 for the year 1985 (Figure 10) can be easily identified with areas affected by fires, as it is the only perturbation that can produce such low values of reflectance. Figures 8, 9, and 10 show clearly the high interannual variability associated to savanna fires, but it is much smaller than the seasonal cycle of surface

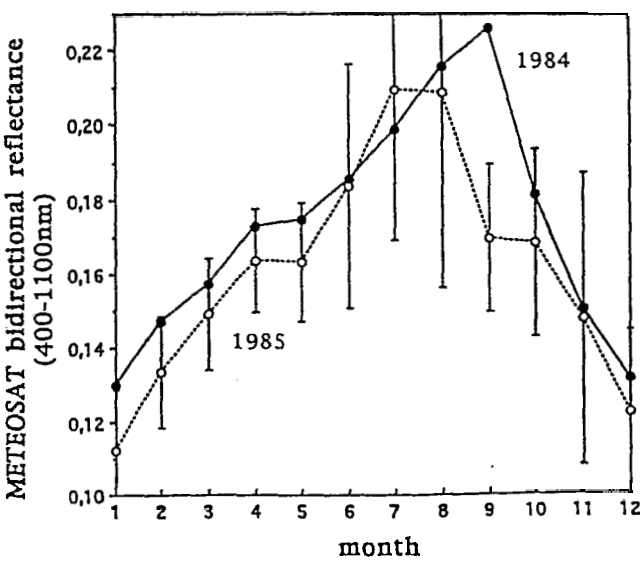

Figure 9. Seasonal variation of bidirectional reflectances observed by Meteosat over the area covered by the grid box of the GCM for the years 1984 and 1985. Bars are standard deviations associated to the spatial variance and are only given for the year 1985 for legibility.

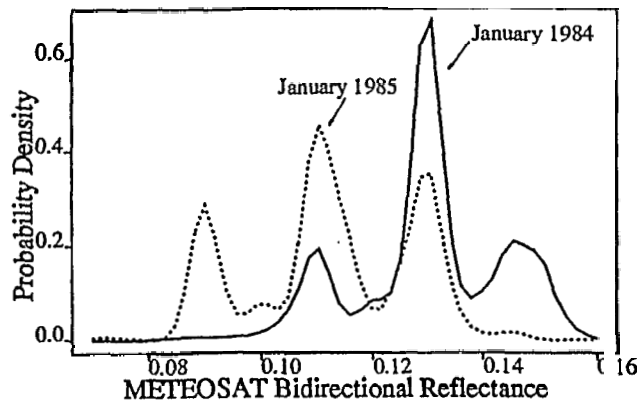

Figure 10. Probability density function of surface bidirectional reflectances observed by Meteosat over the GCM grid box in January 1984 and 1985.

reflectance. At all scales considered here, fires appear as an important pertubation in the West African humid savanna zone.

Savanna fire is a potentially important source of error between simulated and observed surface processes at the regional scale because it affects large areas each year. *Menaut et al.* [1991] noted that the burned area each year represents 25 to 50% of the total land surface in the Sudan zone and 60-80% in the Guinea zone. A global survey of surface reflectance using Meteosat shortwave channel data (400-1100 nm) has shown that at the continental scale humid savanna zones are characterized by low reflectance values during the dry season [*Arino et al.*, 1991,1992]. These low values have to be interpreted today as the impact of savanna fires.

Absorbed radiation at the surface. Absorbed radiation is defined as

$$E_a = (1 - a)R_{s\downarrow} + \epsilon R_{l\downarrow} \qquad (7)$$

where ϵ is the emissivity which is in this case assumed to be constant and equal to unity. Figure 11 compares the annual variations in: (1) absorbed radiation simulated by the GCM over savannas with their prescribed albedo, (2) absorbed radiation recalculated from the simulated incoming radiation and the measured albedo, and (3) the absorbed radiation observed in Lamto. The second calculation was performed in order to estimate the impact of the errors in the prescribed albedo on the absorbed energy. The absorbed radiation simulated by the GCM was much larger than that observed in Lamto. Three types of discrepancies can be distinguished: (1) For the months March to May and October to December the cause of error was the simulated incoming radiation. The difference between the prescribed and the observed albedo had only a minor impact on the absorbed radiation. (2) During the month of June the difference in absorbed radiation was a result of the mismatch of albedos. If the cause of the different albedos would be the variability within the savanna biome then we have to consider that the absorbed radiation simulated by the GCM matched observations. (3) In January and

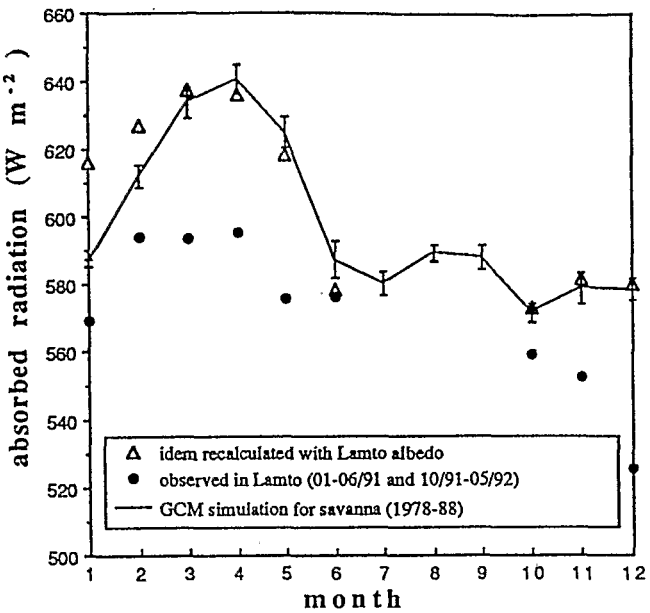

Figure 11. Comparison between absorbed radiation as observed in Lamto, computed by the LMD-GCM for the savanna of the grid box and recomputed with the albedo observed in Lamto.

February the difference in absorbed radiation resulted both from a poor simulation of incoming radiation and from the mismatch of albedos. In fact, the discrepancy is reinforced when the measured albedo is used.

These results show that during most of the year, the simulated absorbed energy was erroneous due to the overestimation of the incoming radiation. In January and February, not representing the impact of bushfires on albedo induced an error in absorbed energy that in our case reduced the overestimation of absorbed radiation. We can conclude that the discrepancy between observed and prescribed savanna albedos had a smaller effect on the simulated absorbed energy than the overestimation of incoming radiation, except for the period of bushfires.

5.3. Outgoing Longwave and Net Radiation

When comparing the measured and modeled outgoing longwave radiation, we have to take into account the identified error in absorbed radiation. We thus consider the ratio of outgoing longwave and absorbed radiation. Figure 12 shows that the temporal evolution of this ratio in the model is similar to the one observed at Lamto. It can be noted that for a same amount of absorbed energy the model would restitute to the atmosphere a smaller part, as upward longwave radiation, but this discrepancy never exeeds 10%. The difference is induced by distinct energy budgets at the surface in Lamto and the GCM grid box, but can this be interpreted as an error of the model if the problem of sub grid scale heterogeneity is taken into account?

In the case of albedo and absorbed radiation we were able to deal with the problem of sub grid scale variability by recomputing the values for savannas in the GCM and compare them to observations in Lamto. If one wants to analyze upward longwave or net radiation along the same lines, one has to have access to the temperature and turbulent fluxes over the savanna biome in the GCM. This means that the land surface scheme should compute an independent energy budget for each biome. SECHIBA already computes evaporation for each vegetation type and averages the fluxes. It is insufficient because temperature is still computed over the entire grid box and thus the same net radiation is available to all vegetation types. In the current state of SECHIBA it is impossible to do a fair comparison of the simulated surface energy budget with point observations.

6. Conclusion

Comparing small-scale (local) measurements of surface/atmosphere exchanges to GCM simulations necessitates coping with the heterogeneity of vegetation types within GCM grid boxes. A potential solution is to treat surface processes separately for each biome and thus compare observations with the corresponding biome in the GCM. Distinguishing different biomes on a GCM grid box for modeling surface processes or comparing the model outputs to observations relies on the hypothesis that they are functional units. This is equivalent to the assumption that within a biome all plots have characteristics which are statistically comparable because a simple statistical distribution encompasses all elements of the biome.

This approach is used in this paper to compare measured albedo and absorbed radiation at the surface in Lamto with values computed in the LMD-GCM over

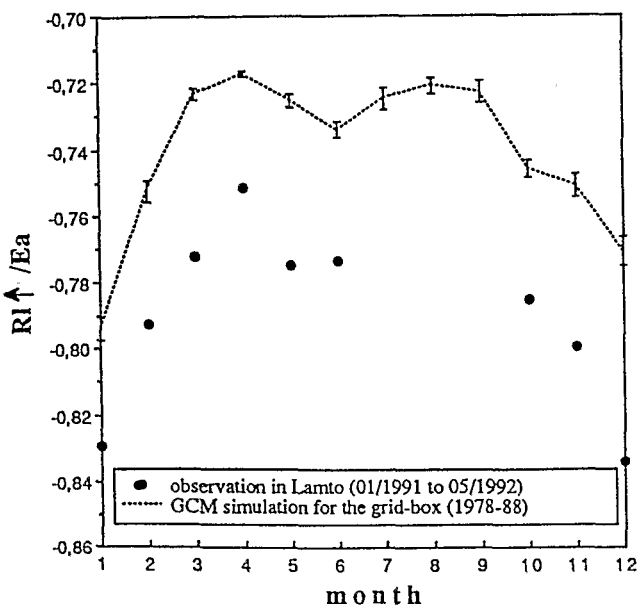

Figure 12. Comparison of the ratio between upward longwave radiation and absorbed energy observed in Lamto from January 1991 to May 1992 and simulated by the LMD-GCM over the 1978-1988 period.

moist savannas. The main conclusions are the following: (1) Savanna fire is a perturbation which affects the surface properties on a scale comparable with the size of GCM grid boxes. (2) The specification of the albedo for moist savannas from the climatology [*Dorman and Sellers*, 1989] used in the LMD-GCM seems to be inadequate and induces an error over the GCM grid box. This discrepancy is due to the fact that the phenology of this biome, driven by a major perturbation (savanna fire), is not taken into account in the data set used by the model. Sensitivity experiments have to be done to test if this information has a significant impact on the simulation of surface/atmosphere interaction, as far as burned savannas are concerned. (3) The incoming shortwave radiation at the surface is strongly overestimated by the GCM. Such an overestimation seems to be common at least at low latitudes in several GCMs. A comparison experiment of surface fluxes observed and simulated by the National Center for Atmospheric Research Community Climate Model over the Amazon Basin [*Dickinson*, 1989] has outlined a significant difference between model simulations and observations. *Shuttleworth and Dickinson* [1989] have pointed out that incoming solar and net radiation were much higher in the simulation, without identifying precisely the major cause among several potential ones: aerosol absorption of shortwave radiation, cloud albedo, mean cloudiness or clear-sky absorption of shortwave radiation. Furthermore, *Garrat* [1993] has shown that both the National Meteorological Center and the United Kingdom Meteorological Office models also overestimate net radiation in the same area. This discrepancy seems to occur also during the summer in high latitudes [*Garratt et al.*, 1993]. In this study, further investigations indicated that the cloudy system albedo is not the source of discrepancy but that the major reason is the bad simulation of clear-sky radiation at the surface (and probably the simulated absorber profiles).

The overestimation of the incoming shortwave radiation at the surface and the deficiencies in the climatology of albedo contribute to the discrepancy that was shown for the absorbed energy.

Acknowledgments. The two first authors are greatly indebted to Katia Laval for numerous discussions and her helpful comments and to one of the anonymous reviewers for his valuable suggestions. We express our gratitude to R. Vuattoux, director of the Lamto Ecological Research Station, for all the facilities he offered us in the field and to J.L. Tireford, director of the Lamto Geophysical Research Station, for making available climatological data. The authors are also grateful to J.Y. Pontailler (Laboratoire d'Ecologie Végétale de Paris Sud) for his help during instrument calibration and E. Birchfield for reviewing the English.

References

Andreae, M. O., Biomass burning: Its history, use, and distribution and its impact on environmental quality and global climate, in *Global Biomass Burning: Atmospheric, Climatic and Biospheric Implications*, edited by J. Levine, pp. 133–142, 1991.

Arino, O., G. Dedieu, and P. Y. Deschamps, Accuracy of satellite land surface reflectance determination, *J. Appl. Meteorol.*, *30*, 960–971, 1991.

Arino, O., G. Dedieu, and P. Deschamps, Determination of land surface spectral reflectances using Meteosat and NOAAA/AVHRR short channel data, *Int. J. Remote Sens.*, *13*, 2263–2287, 1992.

Barkstrom, B., and G. Smith, The Earth Radiation Budget Experiment (ERBE), *Bull. Am. Meteorol. Soc.*, *65*, 1170–1185, 1984.

Bony, S., *Analyse de l'impact des nuages et de la vapeur d'eau sur le cycle saisonnier du bilan radiatif terrestre; Implications pour la sensibilité climatique*, Ph.D. thesis, Univ. of Paris, 1993.

Brunt, D., Notes on radiation in the atmosphere, *Q. J. R. Meteorol. Soc.*, *58*, 389–420, 1932.

Charney, J. G., W. J. Quirk, S.-H. Chow, and J. Kornfield, A comparative study of the effects of albedo change on drought in semi-arid regions, *J. Atmos. Sci.*, *34*, 1366–1385, 1977.

De Abreu, L. D., Y. Viswanadham, and A. O. Manzi, Energy flux partioning over the Amazon forest, *Theor. Appl. Climatol.*, *39*, 1–16, 1988.

Dedieu, G., P. Y. Deschamps, Y. H. Kerr, and P. Raberanto, A global survey of surface climate parameters from satellite observations: Preliminary results over Africa, *Adv. Space Res.*, *7*, (11), 129–137, 1987.

Dickinson, R. E., Implications of tropical deforestation for climate: A comparison of model and observational description of surface energy and hydrological balance, *Philos. Trans. R. Soc. London.*, *324*(B), 423–431, 1989.

Dickinson, R. E., A. Henderson-Sellers, P.J. Kennedy, and M. F. Wilson, Biosphere-atmosphere transfer scheme (BATS) for the NCAR Community Climate Model, *Tech. Rep.*, Natl. Cent. for Atmos. Res. Boulder, Colo., 1986.

Dorman, J. L., and P. J. Sellers, A global climatology of albedo, roughness length and stomatal resistance for atmospheric general circulation models as represented by the simple biosphere model(SIB), *J. Appl. Meteorol.*, *28*, 833–855, 1989.

Ducoudré, N., K. Laval, and A. Perrier, SECHIBA, a new set of parametrizations of the hydrologic exchanges at the land/atmosphere interface within the LMD atmospheric general circulation model, *J. Clim.*, *6*(2), 248–273, 1993.

Fouquart, Y., and B. Bonnel, Computation of solar heating of the earth's atmosphere: A new parametrization, *Beitr. Phys. Atmos.*, *53*(1), 35–62, 1980.

Garratt, J. L., Sensitivity of climate simulations to the land-surface and atmospheric boundary-layer treatments–A review, *J. Clim.*, *6*(3), 419–449, 1993.

Garratt, J. L., P. B. Krummel, and E. A. Kowalczyk, The surface energy balance at local and regional scales–A comparison of general circulation model re-

sults with observations, *J. Clim.*, *6*(6), 1090–1109, 1993.

Gash, J. H. C., J. S.Wallace, C. R. Lloyd, A. J. Dolman, M. V. K. Sivakumar, and C. Renard, Measurements of evaporation from fallow sahelian savannah at the start of the dry season, *Q. J. R. Meteorol. Soc.*, *117*, 749–760, 1991.

Gornitz, V., and NASA, A survey of anthropogenic vegetation changes in West Africa during the last century–Climatic implications, *Clim. Change*, *7*, 285–325, 1985.

Laval, K., and L. Picon, Effect of a change of the surface albedo of the Sahel on climate, *J. Atmos. Sci.*, *43*, 2418–2429, 1986.

Le Treut, H., and Z.-X. Li, Sensitivity of an atmospheric general circulation model to prescribed SST changes: Feedback effects associated with the simulation of cloud optical properties, *Clim. Dyn.*, *5*, 175–187, 1991.

Matthews, E., Prescription of land-surface boundary conditions in GISS GCM II: A simple method based on high-resolution vegetation data bases, *NASA Tech. Memo.*, *86096*, 1984.

Menaut, J.-C., The vegetation of African savannas, in *Ecosystems of the World*, edited by F. Bourlière, pp. 109–149, Elsevier, New York, 1983.

Menaut, J.-C., and J. César, Structure and primary productivity of Lamto savannas, Ivory Coast, *Ecology*, *60*(6), 1197–1210, 1979.

Menaut, J.-C., L. Abbadie, F. Lavenu, P. Loudjani, and A. Podaire, Biomass burning in West African savannas, in *Global Biomass Burning: Atmospheric, Climatic and Biospheric Implications*, edited by J. Levine, pp. 133–149, 1991.

Mintz, Y., The sensitivity of numerically simulated climates to land-surface boundary conditions, in *The Global Climate*, edited by H. J. T., Cambridge University Press, New York, 1984.

Monteith, J. L., Solar radiation and productivity in tropical ecosystems, *J. Appl. Ecol.*, *2*, 747–766, 1972.

Monteny, B. A., *Contribution à l'étude des interactions végétation-atmosphère en milieu tropical humide. Importance du rôle du système forestier dans le recyclage des eaux de pluies*, Ph.D. thesis, Univ. of Paris, 1987.

Monteny, B. A., Relevé des observations climatiques à banizoumbou, tech. rep., Inst. Fr. de Rech. Sci. pour le Dev. en Coop., Montpellier, 1992.

Monteny, B. A., and A. Casenave, The tropical contribution to the hydrological budget in tropical West Africa, *Ann. Geophys.*, *7*(4), 427–436, 1989.

Monteny, B. A., and G. Gosse, Trouble atmosphérique et rayonnement solaire en basse Côte d'Ivoire, *Agr. Meteorol.*, *19*, 121–136, 1978.

Morcrette, J.-J., L. Smith, and Y. Fouquart, Pressure and temperature dependence of the absorption in longwave radiation parametrizations, *Beitr. Phys. Atmos.*, *59*, 455–468, 1986.

Oguntoyinbo, J. S., Reflection coefficient of natural vegetation, crops and urban surfaces in Nigeria, *Q. J. R. Meteorol. Soc.*, *96*, 430–441, 1970.

Pinker, R. T., O. E. Thompson, and T. F. Eck, The albedo of a tropical evergreen forest, *Q. J. R. Meteorol. Soc.*, *106*, 551–558, 1980.

Polcher, J., and K. Laval, A statistical study of regional impact of deforestation on climate of the LMD-GCM, *Clim. Dyn.*, in press, 1994.

Polcher, J., et al., Le cycle 5 du modèle de circulation générale du LMD., *Tech. Rep.*,*LMD Internal Note Nb 170*, Paris, 1991.

Rahman, H., and G. Dedieu, SMAC: A simplified method for the atmospheric correction of satellite measurements in the solar spectrum, *Int. J. Remote Sens.*, *15*, 123–143, 1994.

Sadourny, R., and K. Laval, January and July performance of the LMD general circulation model, in *New Perspectives in Climate Modelling*, edited by A. L. Berger and C. Nicolis, pp. 173–197, Elsevier Science Publishers, New York, 1984.

Sellers, W., *Physical Climatology*, University of Chicago Press, Chicago Ill., 1965.

Sellers, P. J., Y. Mintz, Y. C. Sud, and A. Dachler, A simple biopshere model (SiB) for use within general circulation models, *J. Atmos. Sci.*, *46*(6), 505–531, 1986.

Shuttleworth, J. W., Evaporation from amazonian rainforest, *Proc. R. Soc. London*, *233*, 321–346, 1988.

Shuttleworth, J. W., and R. E. Dickinson, Comments on "Modelling tropical deforestation: A study of GMC land-surface parameterizations" by R.E.Dickinson and A.Henderson-Sellers, *Q. J. R. Meteorol. Soc.*, *115*, 1177–1179, 1989.

Shuttleworth, J. W., et al., Observations of radiation exchange above and below Amazonian forest., *Q. J. R. Meteorol. Soc.*, *110*, 1163–1169, 1984.

Shuttleworth, J. W., et al., Eddy correlation measurements of energy partition for Amazonien forest, *Q. J. R. Meteorol. Soc.*, *110*, 1143–1162, 1988.

Van de Griend, A. A., M. Owe, M. Groen, and M. P. Stoll, Measurement and spatial variation of thermal infraread surface emissivity in a savanna environment, *Water Res. Res.*, *27*(3), 371–379, 1989.

White, F., La végétation de l'Afrique, Carte, Inst. Fr. de Rech. Sci. pour le Dev. en Coop.-UNESCO, UNESCO, Paris, 1986.

G. Dedieu, LERTS, Unité mixte CNES-CNRS, 18 av. E. Belin, 31055 Toulouse, France.

X. Le Roux, and J.C. Menaut, Ecole Normale Supérieure (ENS) Laboratoire d'Ecologie, URA 258 CNRS, 46 rue d'Ulm, 75230 Paris Cedex 05, France. xleroux@biologie.ens.fr

B.A. Monteny, Laboratoire de Bioclimatologie, Institut Francais de Recherche Scientifique pour le Developpement en Cooperation (ORSTOM), 911 av. Agropolis BP 5045 , 34032 Montpellier, France.

J. Polcher, Laboratoire de Météorologie Dynamique du CNRS,ENS,24 rue Lhomond, 75231 Paris Cedex 05, France. polcher@lmd.ens.fr

(Received May 7, 1993; revised June 13, 1994; accepted June 13, 1994.)